Nonuniform Array Design for Robust Millimeter-Wave MIMO Links

Eric Torkildson, Colin Sheldon, Upamanyu Madhow, and Mark Rodwell
Department of Electrical and Computer Engineering
University of California, Santa Barbara
Santa Barbara, CA 93106
Email: etorkild@ece.ucsb.edu

***Abstract*—Spatial multiplexing for millimeter (mm) wave line of sight (LOS) links potentially enables data rates of the order of 10-100 Gbps. Most prior work in this area has focused on uniform transmit and receive arrays, for which it is known that the spatial responses seen by different transmitters can be made orthogonal by choosing the antenna spacing appropriately as a function of range and wavelength. In this paper, we show that variations in range can cause significant degradation in performance for such uniformly spaced arrays optimized for a given range, due to the appearance of high correlations between the spatial responses for different transmitters (and hence rank deficiency in the MIMO channel matrix) as a function of range. We then demonstrate that optimized nonuniform arrays alleviate this problem by keeping correlations between spatial responses small over a significantly larger set of ranges than is possible with uniform spacing.**

I. Introduction

In this paper we consider the design of nonuniform antenna arrays for use with line-of-sight (LOS) multiple-input multiple-output (MIMO) links. Prior work in this area of LOS MIMO has focused on the design of uniform arrays. We propose that nonuniform arrays offer robust performance over a larger set of link range than a uniform array of identical length. Our treatment of the problem is placed in the context of the mm wave MIMO architecture, a high speed point-to-point wireless link designed to achieve an order of magnitude increase in data rates over current systems.

The mm wave MIMO architecture operates in the 60 GHz or 70-95 GHz frequency bands where large swathes of bandwidth are available on an unlicensed or semi-unlicensed basis [1]. Aggregate data rates of 40+ Gbps are achieved by transmitting several independent 5-10 Gbps data streams in parallel over multiple antennas, as shown in Fig. 1.

Spatial multiplexing, the transmission of multiple independent signals in parallel over a multi-antenna link, has been studied extensively in the literature since the landmark papers of Foschini [2] and Telatar [3]. The bulk of work in this area has addressed spatial multiplexing in rich scattering environments, where the complex channel gains can be modeled as random variables. A mm wave MIMO link, however, operates primarily over a line-of-sight (LOS) environment where the channel coefficients are largely deterministic and specified by the array geometry. Spatial multiplexing over a LOS channel is possible given appropriate spacing between antenna elements [4]. The required inter-element spacing scales as $\sqrt{R\lambda}$ where R is the range and λ is carrier wavelength. At mm wavelengths, spatial multiplexing can be achieved in a LOS environment using moderately sized arrays.

Given knowledge of the link range and carrier frequency, a uniform linear or rectangular array can be designed that provides a spatially uncorrelated MIMO channel [5], [6]. However, these arrays must be separated by the prescribed distance for the channel to remain uncorrelated. In many scenarios of practical interest, a link may be deployed over an actual link range that differs from the nominal link range. When this occurs, the use of uniformly spaced arrays may result in a highly correlated channel. We seek an array design that provides acceptable performance over the largest possible interval surrounding the nominal link range. The main contribution of this paper is to demonstrate that nonuniform arrays can be far superior to uniform arrays in this regard.

Prior work in the area of nonuniform array design has addressed array pattern synthesis, with early contributions by King [7] and Harrington [8]. These papers consider the far-field array radiation pattern, which assumes a planar wave approximation. In this work, the geometry of both the transmit and receive arrays must be considered jointly, and the plane wave approximation must be abandoned in favor of the more accurate spherical wave propagation model. The spherical wave model is more appropriate due to the small carrier wavelength and moderate antenna spacings considered here.

Multi-antenna architectures operating at mm wave frequencies have previously been studied in the literature. Notably, the authors of [9] outlined the challenges and various solutions associated with building low-cost, high data-rate 60 GHz wireless links. The antenna array in their proposed architecture are used for beamforming, in order to boost gain and reduce multipath. The architecture proposed here, on the other hand, uses multiple antennas for spatial multiplexing.

The paper is organized as follows. We review the mm-wave MIMO architecture and basic geometry of LOS MIMO channels in Section II. In Section III, we provide a brief derivation of the linear Rayleigh-spaced array and investigate its performance when used at various link ranges. The specific

This research was supported in part by the National Science Foundation under grants ECS-0636621, CCF-0729222 and CNS-0832154.

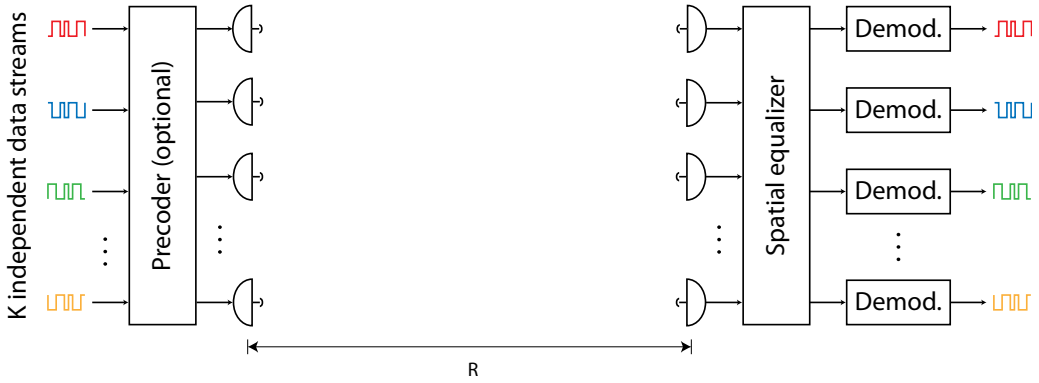

Fig. 1. Overview of the proposed mm wave MIMO system. Both the transmit and receive nodes include an N-element antenna array. R denotes the link range.

link ranges at which the channel becomes spatially correlated are identified. This motivates our discussion of the nonuniform array in Section IV. An optimization metric is provided, along with several examples of optimized arrays. Concluding thoughts and discussions of future work are provided in Section V.

II. Background

This section presents an overview of the mm wave MIMO system, a scalable multi-antenna architecture capable of spatial multiplexing over a line-of-sight wireless channel. Consideration of this system and its constraints will provide a context for later discussion of array optimization. The section also includes a review of the LOS MIMO channel model.

A. The millimeter-wave MIMO architecture

As mentioned above, the mm wave MIMO architecture is designed to provide an order of magnitude increase in data rates compared to existing wireless links. To achieve these rates, the system exploits the abundant bandwidth available at mm wave frequencies. In the United States, the mm wave spectrum includes 7 GHz of unlicensed bandwidth available in the 60 GHz band, 10 GHz of semi-unlicensed bandwidth available in the 71-76 GHz and 81-86 GHz bands, and 3 GHz of unlicensed bandwidth available in the 92-95 GHz band. Although bandwidth is plentiful at these frequencies, it is difficult to generate large amounts of transmit power using emerging silicon implementations. This drives us towards power-efficient (i.e. small constellation) communication over large bands. This is in contrast to systems operating at lower frequencies, which typical favor spectrally efficient communication over relatively narrow bands (20-40 MHz).

Fig. 1 shows a high level diagram of the mm wave MIMO architecture. The system transmits K independent 5-10 Gbps data streams in parallel using multiple antennas at the transmitter and receiver to achieve the desired aggregate rate of 40+ Gbps. Highly directive antennas are typically used at mm wave frequencies to overcome high attenuation loss and conform to FCC regulation. Over the 71-76 GHz or 81-86 GHz bands, for instance, a minimum directivity of 43 dBi and a maximum beamwidth of 1.6° is required by the FCC. Due to high multipath attenuation and narrow beamwidths, the mm wave MIMO cannot rely on multipath scattering to provide a spatially uncorrelated channel. Instead, we require that antenna elements are spaced sufficiently far apart. Spacing requirements are discussed detail in Section III.

We assume herein that no precoding is performed. Although precoding is required for eigenchannel transmission, a capacity-achieving multiplexing scheme [10], mm wave hardware constraints would severely limit this approach. Specifically, capacity is achieved through eigenchannel transmission by allocating more power to strong eigenchannels via water-filling. However, the dynamic limited range of current mm wave hardware constrains the amount of power allocation that is possible. Further, we are constrained to small constellations (i.e. BPSK, QPSK) that fall short of capacity given a high SNR channel. Thus, we have little to gain by performing precoding at the cost of added complexity.

We further assume that a zero-forcing (ZF) filter, also known as a decorrelating receiver, serves as the spatial equalizer. A linear equalization scheme such as this can be implemented in analog hardware as a network of variable-gain amplifiers and tunable phase arrays operating at IF. An analog processing approach is favorable because current analog-to-digital converters are incapable of sampling a signal with 5-7 GHz bandwidth at sufficient precision to perform accurate DSP-based spatial equalization. This approach therefore permits scaling to larger bandwidths and higher data rates.

Experimental results for a two-channel prototype and a four-channel prototype of the mm-wave MIMO architecture have been reported in [11] and [12], respectively. These results verify the feasibility of the proposed scalable architecture as well as the applicability of the LOS MIMO channel model, described next.

B. LOS MIMO channel model

Consider a point-to-point LOS link with an N-element antenna array at each node. Assuming no temporal intersymbol interference, which is a reasonable approximation given the narrow beams radiated by highly directive antennas, the $N \times 1$

received signal vector $\mathbf{r}$ is given by

$$\mathbf{r} = \mathbf{H}\mathbf{s} + \mathbf{n} \tag{1}$$

where $\mathbf{s}$ is the $N \times 1$ transmitted vector, $\mathbf{n}$ is an $N \times 1$ zero mean circularly symmetric complex white Gaussian noise vector with covariance $R_n = 2\sigma^2\mathbf{I}_N$ and $\mathbf{I}_N$ is the $N \times N$ identity matrix. $\mathbf{H}$ is the $N \times N$ channel matrix with entries $h_{m,n}$ corresponding to the complex channel gain from the nth transmit element to the mth receive element. Assuming a strictly LOS channel with no signal path loss (the loss is accounted for in the link budget), the elements of the channel matrix are given by $\tilde{h}_{m,n} = e^{-j\frac{2\pi}{\lambda}p(m,n)}$, where $p(m,n)$ is the path length from nth transmit element to the mth receive element. Only the relative phase shifts between elements of $\mathbf{H}$ are of interest, so for notational convenience we normalize $\tilde{h}_{m,n}$ by a factor of $e^{j\frac{2\pi}{\lambda}R}$, resulting in

$$h_{m,n} = e^{-j\frac{2\pi}{\lambda}(p(m,n)-R)} = e^{-j\frac{2\pi}{\lambda}\Delta p(m,n)} \tag{2}$$

where $\Delta p(m,n) = p(m,n) - R$ and λ is the carrier wavelength.

Specializing to linear arrays aligned to the broadside of each other, let $\mathbf{x} = [x_1, x_2, \ldots, x_N]$ specify the positions of the N array elements relative to the top of the array, i.e. $x_1 = 0$ and $x_N = L$, where L is the total length of the array. $\Delta p(m,n)$ can now be expressed as

$$\Delta p(m,n) = \sqrt{(x_m - x_n)^2 + R^2} - R \approx \frac{(x_m - x_n)^2}{2R} \tag{3}$$

with the approximation holding for $|x_m - x_n| \ll R$. The entries of the channel matrix are given by

$$h_{m,n} \approx e^{-j\frac{\pi}{R\lambda}(x_m - x_n)^2} \tag{4}$$

Given the values of λ and R, it is possible to position the array elements such that each column of $\mathbf{H}$ is orthogonal to every other column. This allows all N signals to be recovered (using, for instance, the zero-forcing equalizer) without suffering performance degradation due to spatial interference. In the next section, we review an array design which meets this criteria.

III. The Rayleigh-spaced Array

The Rayleigh spacing criterion specifies the minimum inter-element spacing that guarantees a spatially uncorrelated channel. The criterion is dependent on N, λ, and R. In practice, the precise link range R may be unknown during the design and manufacture of an array, and so we will analyze the link when R deviates from the predicted value.

A. Derivation of the Rayleigh spacing criterion

Consider the simple example of two N-element uniform linear arrays (ULAs) aligned to the broadside of each other, as shown in Fig. 1. Assume the link range is known, and given by R_o. The spacing between adjacent elements is d, resulting in a position vector of $\mathbf{x} = [0, d, 2d, \ldots, (N-1)d]$. The path length difference (relative to R_o) is given by

$$\Delta p(m,n) \approx (m-n)^2 \frac{d^2}{2R_o} \tag{5}$$

where $(m-n)d \ll R_o$. The entries of the channel matrix are given by

$$h(m,n) \approx e^{-j(m-n)^2\frac{\pi d^2}{\lambda R_o}} = e^{-j(m-n)^2\phi} \tag{6}$$

where $\phi = (\pi d^2)/(\lambda R_o)$ is the phase difference between neighboring elements. The correlation between the receive array responses to the kth transmit element and the mth transmit element, with $k \neq m$, is given by

$$\begin{aligned}\rho(k,m) &= \frac{|\mathbf{h}_k^H \mathbf{h}_m|}{\|\mathbf{h}_k\|\|\mathbf{h}_m\|} \\ &= \frac{1}{N}\left|\sum_{n=0}^{N-1} e^{-j\left((k-n-1)^2-(m-n-1)^2\right)\phi}\right| \\ &= \frac{1}{N}\left|\frac{\sin(N(k-m)\phi)}{\sin((k-m)\phi)}\right| \\ &= \rho(k-m), \quad k,m \in \{1,2,\ldots,N\}\end{aligned} \tag{7}$$

where $\mathbf{h}_k$ is the kth column of $\mathbf{H}$. From Eq. (7), we observe that the correlation between receive array responses is driven to zero when $N\phi = \pi$. Substituting this result into Eq. (6), we obtain the optimal uniform spacing

$$d_{\mathrm{R}} = \sqrt{\frac{R_o\lambda}{N}} \tag{8}$$

which is identical to the familiar Rayleigh criterion, the diffraction-limited resolution of an optical system. Let $\mathbf{x}_{\mathrm{u}} = [0, d_{\mathrm{R}}, 2d_{\mathrm{R}}, \ldots, (N-1)d_{\mathrm{R}}]$ denote the position vector of an N-element Rayleigh-spaced array. A 4-element array operating at 75 GHz over 100 m satisfies the Rayleigh criterion at $d_{\mathrm{R}} = 0.316$ m and the total array length is $L = (N-1)d_{\mathrm{R}} = 0.95$ m. If the link range is increased to 1 km, the Rayleigh criterion spacing increases to 1m, for a total array size of $L = 3$ m. Eq. (8) also specifies the optimal element spacing of $N \times N$ uniform square arrays aligned broadside [6]. Thus a Rayleigh-spaced 4×4 square array would occupy an area of 3 m $\times$ 3 m.

A more detailed derivation of the optimal uniform spacing is provided by Bohagen et al. [13] [5]. The authors consider linear and rectangular arrays facing arbitrary directions.

B. Spatial correlation at non-optimal link ranges

When the Rayleigh criterion is met, the channel matrix is scaled unitary and the (noisy) transmitted signal vector $\mathbf{s}$ can be recovered using spatial equalization techniques without suffering degradation of the signal-to-noise (SNR) ratio. However, when the link operates at a range $R \neq R_o$, correlation will be present among columns of $\mathbf{H}$ and spatial equalization leads to increased noise power. From Eq. (7), note that the correlation $\rho(k-m)$ is dependent on R through $\phi = \frac{\pi d^2}{\lambda R} = \frac{\pi R_o}{NR}$.

To demonstrate, we consider a 4-element linear array link with a carrier frequency of $f = 75$ GHz. Fig. 2 plots the correlation $\rho(k-m)$ of the receive array responses to transmit elements k and m as the link range is varied from 200 m to 2 km. $\rho(1)$ is the correlation between adjacent columns

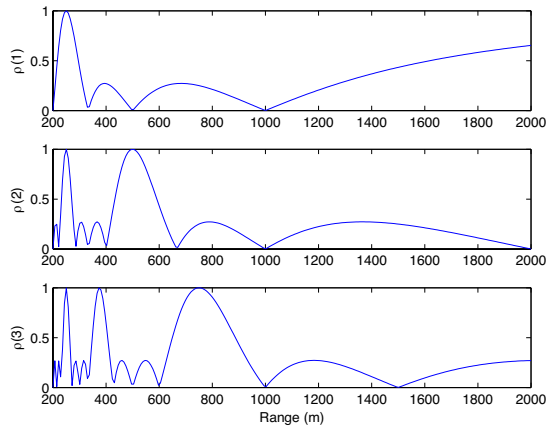

Fig. 2. Correlation among columns of $\mathbf{H}$ as a function of link range for a 4-element Rayleigh-spaced array.

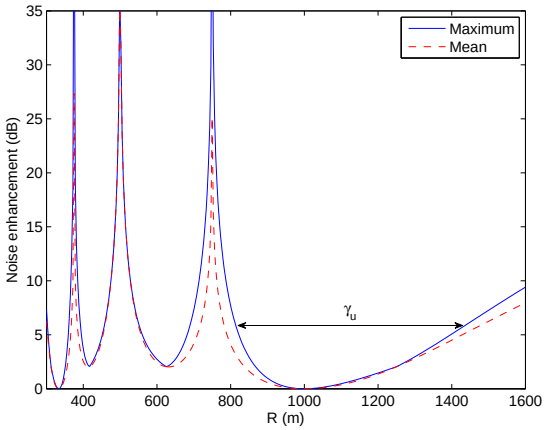

Fig. 3. Maximum and mean noise enhancement as a function of range for a 4-element Rayleigh-spaced array.

of $\mathbf{H}$, i.e. correlation among the receive array responses to neighboring transmit elements. Similarly, $\rho(2)$ corresponds to transmit elements separated by $2d$. Hence, it represents correlation between responses to the first and third transmit elements, or the second and fourth transmit elements. Finally, $\rho(3)$ corresponds to transmit elements separated by distance $3d$, i.e. the outermost elements transmit array.

At some values of R, correlation between two or more columns of $\mathbf{H}$ approaches unity, in which case the channel matrix becomes ill-conditioned. For instance, when $R = \frac{d^2}{\lambda} = \frac{R_{\mathrm{RC}}}{N}$ the phase difference between adjacent receive elements is $\phi = \pi$ and $\mathbf{H}$ becomes rank one. In general, from Eq. (7) we find that $\rho(n)$ goes to unity whenever R takes on the values

$$R = \frac{n}{kN} R_o, \quad k = 1, 2, 3, \ldots \tag{9}$$

for $n = 1, 2, \ldots, N-1$. This equation specifies the link ranges at which $\mathbf{H}$ becomes ill-conditioned for both Rayleigh-spaced N-element ULAs and Rayeleigh-spaced $N \times N$-element square arrays. According to Eq. (9), as R deviates from R_o, correlation among columns of $\mathbf{H}$ first reaches unity at $R = \frac{N-1}{N} R_o$. At this distance, the receive array responses to the outermost transmit elements become perfectly correlated.

C. Noise enhancement at non-optimal link ranges

To assess the impact of spatial correlation on system performance, we will consider the output of a zero-forcing spatial equalizer. The ZF equalizer cancels out spatial interference entirely by filtering the received signal vector by the pseudo-inverse of the channel matrix, given by

$$\mathbf{C}_{\mathrm{ZF}} = \mathbf{H}^{\dagger} = \mathbf{H}^H (\mathbf{H}\mathbf{H}^H)^{-1} \tag{10}$$

$\mathbf{H}$ is typically invertible (although possibly ill-conditioned), in which case the pseudo-inverse and inverse coincide. The output of the zero-forcing equalizer is

$$\mathbf{y} = \mathbf{C}_{\mathrm{ZF}} (\mathbf{H}\mathbf{s} + \mathbf{n}) = \mathbf{s} + \tilde{\mathbf{n}} \tag{11}$$

where $\tilde{\mathbf{n}}$ is an $N \times 1$ complex Gaussian noise vector with covariance $2\sigma^2 \mathbf{C}_{\mathrm{ZF}}^H \mathbf{C}_{\mathrm{ZF}}$. The ZF equalizer eliminates spatial interference entirely at the cost of an increase in noise power, referred to as noise enhancement. For a given array configuration $\mathbf{x}$, the noise enhancement incurred by the ith transmitted signal is given by

$$\eta_i(\mathbf{x}, R) = \|\mathbf{h}_i\|^2 \|\mathbf{c}_i\|^2 = N \|\mathbf{c}_i\|^2 \tag{12}$$

where $\mathbf{c_i}$ is the ith column of $\mathbf{C}_{\mathrm{ZF}}$ and the dependence of $\mathbf{c}_i$ on $\mathbf{x}$ and R is implicit. The mean noise enhancement is given by

$$\bar{\eta}(\mathbf{x}, R) = \frac{1}{N} \sum_{i=1}^{N} \eta_i(R) = \sum_{i=1}^{N} \frac{1}{\lambda_i^2} \tag{13}$$

where λ_i are the singular values of $\mathbf{H}$ evaluated at R.

Fig. 3 plots the mean noise enhancement, $\bar{\eta}(\mathbf{x}_{\mathrm{u}}, R)$, and the maximum noise enhancement, $\max_i \eta_i(\mathbf{x}_{\mathrm{u}}, R)$, of the 4-element Rayleigh-spaced array. Note that noise enhancement increases as soon as R deviates from R_o. A link budget analysis suggests that, even under unfavorable weather conditions, the link margin can be set as high as 10 to 20 dB [1]. A portion of the link margin can be allocated to offsetting the effects of noise enhancement. However, the noise enhancement far exceeds the entire link margin at ranges of 375 m, 500 m, and 750 m, i.e. at ranges given by Eq. (9) where the correlation among columns of $\mathbf{H}$ approaches one.

Although other spatial equalization methods (eigenchannel transmission, BLAST, and MMSE) could be considered, these schemes suffer performance degradation at the same link ranges as the ZF receiver due to spatial correlation in the channel. In particular, MMSE and ZF equalization give similar performance at moderate to high SNRs, with the MMSE receiver tending to the ZF receiver asymptotically as the SNR gets large. Thus we focus on noise enhancement throughout as a simple SNR-independent metric of array performance.

In the next section, we consider the use of optimized nonuniform arrays that sacrifice optimality at R_o to provide

acceptable performance over a larger set of link ranges. By breaking the uniformity of the array, the noise enhancement spikes closest to R_o can be avoided.

IV. Optimized nonuniform arrays

Let $[R_1, R_2]$ denote the interval about R_o for which the maximum noise enhancement remains below a given threshold η. Letting $\gamma = R_2 - R_1$, the goal of our optimization will be to find a nonuniform linear array that maximizes γ. The maximum is denoted by γ_o. For comparison, we let γ_u denote the value of our metric when using Rayleigh-spaced uniform arrays. For example, consider the four-element uniform array optimized for $R_o = 1$ km. Setting $\eta = 6$ dB, we have $R_1 = 810$ m and $R_2 = 1440$ m, as shown in Fig. 3. The link will operate reliably given $R \in [810, 1440]$ m, corresponding to $\gamma_u = 630$ m.

A. 4-element nonuniform array analysis

To gain insight into the optimization problem, we begin with 4-element Rayleigh-spaced arrays at both ends of the link. The array is optimized for link range $R_o = 1$ km. Keeping the outer two elements fixed, we allow the inner two elements to shift inward or outward in position by an equal amount, maintaining symmetry about the center of the array. The element positions are given by $\mathbf{x} = [0, \alpha d_R, (3-\alpha)d_R, 3d_R]$, with $\alpha = 1$ corresponding to the original Rayleigh-spaced array.

As shown by Fig. 3, γ_u is limited by the rightmost spike in noise enhancement, which occurs at $3/(4R_o)$. This spike is the result of high correlation between the first and fourth columns of $\mathbf{H}$, corresponding to the outer transmit elements. Allowing the correlation to take on values in $[-1, 1]$, $\rho(1,4)$ can be expressed as a sum of cosines as follows

$$\rho(1,4) = \frac{1}{2}\cos\left(\frac{9\pi R_o}{4R}\right) + \frac{1}{2}\cos\left(\frac{3\pi R_o}{4R}(3+2\alpha)\right) \quad (14)$$

The individual terms and their sum are displayed in the top plot of Fig. 4 for $\alpha = 1$. We observe that $\rho(1,4) = -1$ at 750 m, resulting in a noise enhancement spike as expected. The first term, plotted as a dashed line, is independent of the choice of α while the second term is dependent. We can predict that a good choice of α is one that avoids coinciding positive or negative peaks among the cosine terms in the range interval of interest.

Setting $\eta = 6$ dB, the the metric γ has been computed numerically for $\alpha \in [0, 1.5]$, with the results shown in Fig. 5. We find that the nonuniform array outperforms the Rayleigh-spaced array for any values of α between roughly 0.5 and 1. The optimal value occurs at $\alpha = 0.576$. Although not shown, the correlations $\rho(1,2)$ and $\rho(3,4)$ grow large for $\alpha < 0.5$, resulting in a low value of γ. This is as expected, because the receiver has difficulty resolving the inner and outer elements when they are placed close together.

As shown in the Fig. 4, the optimal value of α maintains ensures that $\rho(3)$ remains small at values of R surrounding R_o. This provides an intuitive notion of what constitutes a good nonuniform array, however, it also highlights the complexity

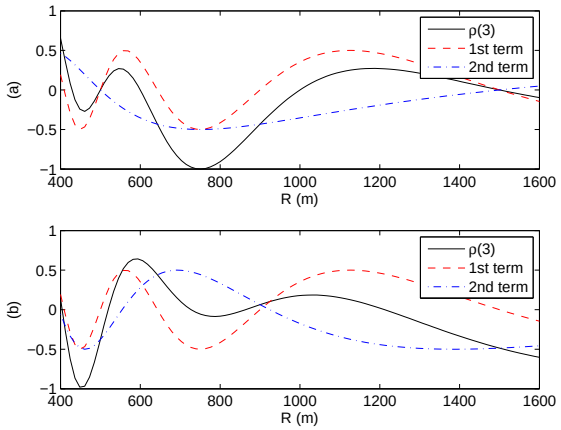

Fig. 4. Correlation $\rho(1,4)$, corresponding to signals from the outermost elements of the transmit array. In the top plot, $\alpha = 1$. In the bottom plot, $\alpha = 0.576$.

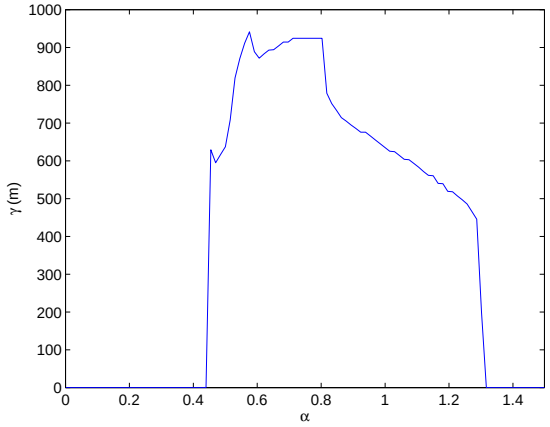

Fig. 5. Optimization metric γ for 4-element array with elements at $\mathbf{x} = [0, \alpha d_R, (3-\alpha)d_R, 3d_R]$.

of the problem. First, the distance between adjacent peaks of each cosine term shrinks as R decreases, thus it becomes increasingly difficult to ensure that peaks do not coincide as R decreases. In fact, even in the optimized case, negative peaks coincide at $R = 500$ m, resulting in a sharp spike in noise enhancement at this range. Second, we have constrained ourselves to a nonuniform array that is symmetric about the center of the array. Asymmetric arrays may perform significantly better, although they are considerably more difficult to characterize analytically.

Based on these factors, we proceed to perform a numerical optimization of asymmetric nonuniform arrays. Because the number of elements in a mm-wave MIMO array is limited by practical constraints on the array's physical size, exhaustive search for optimal positions remains a computationally feasible option.

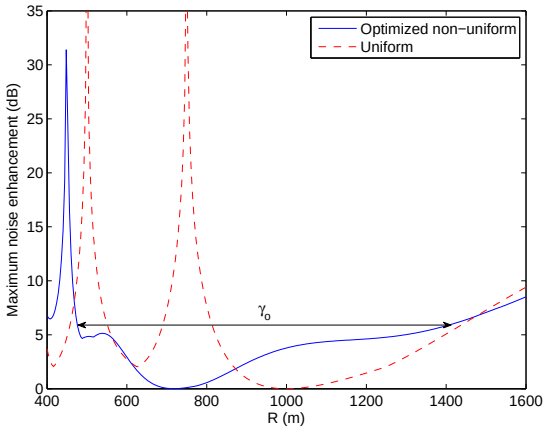

Fig. 6. Maximum noise enhancement as a function of range for an optimized 4-element nonuniform linear array.

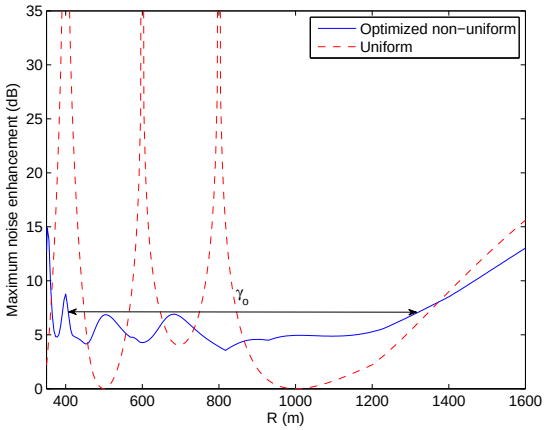

Fig. 7. Maximum noise enhancement as a function of range for an optimized 5-element nonuniform linear array.

TABLE I
ELEMENT POSITIONS IN METERS FOR OPTIMIZED NONUNIFORM ARRAYS

	x_1	x_2	x_3	x_4	x_5	x_6
4 element	0	0.58	2.42	3.00		
5 element	0	0.46	1.94	2.64	3.58	
6 element	0	0.42	1.61	2.67	3.38	4.08

B. Optimization procedure and results

The optimization procedure is first performed on a 4-element array with an expected link range of $R_o = 1$ km. Our optimization goal is to maximize $\gamma = R_2 - R_1$, where $[R_1, R_2]$ is the interval about R_o on which the noise enhancement remains below $\eta = 6$ dB. The array length is fixed at $L = 3$ m, i.e. the length of a 4-element Rayleigh spaced optimized for a 1 km link range. The antenna position vector is given by $\mathbf{x} = [0, x_2, x_3, 3]$ with $x_2 \in [0, 1.5]$ and $x_3 \in [1.5, 3]$. The optimal element positions, determined through exhaustive search, are given by $\mathbf{x} = [0, 0.58, 2.42, 3]$. We note that the optimal nonuniform array is, in this case, symmetric, although symmetry does not hold in general. The noise enhancement of the optimized array is plotted in Fig. 6. γ_o is 941 m, a 49% increase over $\gamma_u = 630$ m.

The procedure was repeated for a 5-element array with η increased to 6.97 dB to account for the additional receive array processing gain provided by the extra array element. Fig. 7 plots the resulting noise enhancement. $\gamma_o = 923$ m, an 85% increase over $\gamma_u = 498$ m. Similarly, a 6-element array was optimized with $\eta = 7.76$ dB. The noise enhancement is plotted in Fig. 8. In this case, $\gamma_o = 918$ m provides a 121% improvement over $\gamma_u = 415$ m. The antenna positions of the three optimized arrays are provided in Table I.

We observe that, although γ_u decreases by roughly 20% with each additional array element, γ_o remains nearly constant. This trend suggests that the benefit of nonuniform optimization grows with increasing N.

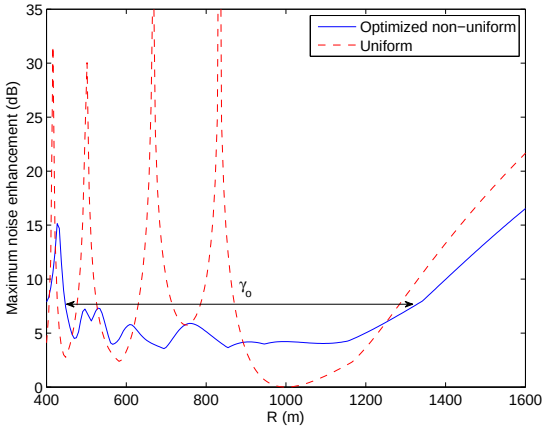

Fig. 8. Maximum noise enhancement as a function of range for an optimized 6-element nonuniform linear array.

V. CONCLUSION

In this paper, we presented a case for the use of nonuniform arrays in LOS MIMO systems. In practice, the precise distance between nodes may be unknown during the array design process. Therefore, we examined how system performance is affected when array size and link range are are not matched according to the Rayleigh spacing criterion. Under a zero-forcing equalization scheme, significant degradation of SNR at the output of the equalizer may occur. Seeking to minimize these effects, alternate array geometries were considered. It was demonstrated that non-uniform antenna spacing can provide acceptable performance over a larger set of link ranges than uniform Rayleigh spacing.

REFERENCES

[1] E. Torkildson, B. Ananthasubramaniam, U. Madhow, and M. Rodwell, "Millimeter-wave MIMO: Wireless links at optical speeds," in *Proc. of 44th Allerton Conference on Communication, Control and Computing*, September 2006.

[2] G. J. Foschini and M. Gans, “On the limits of wireless communications in a fading environment when using multiple antennas,” *Wireless Personal Communications*, vol. 6, no. 3, p. 311, Mar. 1998.
[3] I. E. Telatar, “Capacity of multi-antenna Gaussian channels,” AT&T Bell Lab Internal Tech. Memo., Oct. 1995.
[4] P. Driessen and G. Foschini, “On the capacity formula for multiple input-multiple output wireless channels: a geometric interpretation,” *Communications, IEEE Transactions on*, vol. 47, no. 2, pp. 173–176, Feb 1999.
[5] F. Bohagen, P. Orten, and G. Oien, “Design of optimal high-rank line-of-sight MIMO channels,” *Wireless Communications, IEEE Transactions on*, vol. 6, no. 4, pp. 1420–1425, April 2007.
[6] P. Larsson, “Lattice array receiver and sender for spatially orthonormal MIMO communication,” *Vehicular Technology Conference, 2005. VTC 2005-Spring. 2005 IEEE 61st*, vol. 1, pp. 192–196 Vol. 1, May-1 June 2005.
[7] D. King, R. Packard, and R. Thomas, “Unequally-spaced, broad-band antenna arrays,” *Antennas and Propagation, IRE Transactions on*, vol. 8, no. 4, pp. 380–384, July 1960.
[8] R. Harrington, “Sidelobe reduction by nonuniform element spacing,” *Antennas and Propagation, IRE Transactions on*, vol. 9, no. 2, pp. 187–192, March 1961.
[9] C. Doan, S. Emami, D. Sobel, A. Niknejad, and R. Brodersen, “60 GHz CMOS radio for Gb/s wireless LAN,” in *Radio Frequency Integrated Circuits (RFIC) Symposium, 2004. Digest of Papers. 2004 IEEE*, June 2004, pp. 225–228.
[10] D. Tse, *Fundamentals of Wireless Communication*. Cambridge, UK: Cambridge University Press, 2008.
[11] C. Sheldon, M. Seo, E. Torkildson, M. Rodwell, and U. Madhow, “Four-channel spatial multiplexing over a millimeter-wave line-of-sight link,” *IEEE - MTTS International Microwave Symposium (to be presented at)*, June 2009.
[12] C. Sheldon, E. Torkildson, M. Seo, C. P. Yue, M. Rodwell, and U. Madhow, “Spatial multiplexing over a line-of-sight millimeter-wave MIMO link: A two-channel hardware demonstration at 1.2Gbps over 41m range,” in *38th European Microwave Conference*, October 2008.
[13] F. Bohagen, P. Orten, and G. Oien, “Optimal design of uniform rectangular antenna arrays for strong line-of-sight MIMO channels,” *EURASIP J. Wirel. Commun. Netw.*, vol. 2007, no. 2, pp. 12–12, 2007.